

The diagnosis of brain tuberculoma by ^1H -magnetic resonance spectroscopy

Ky Santy · Phang Nan · Yay Chantana ·
Denis Laurent · David Nadal · Beat Richner

Received: 12 January 2011 / Revised: 21 January 2011 / Accepted: 22 January 2011
© Springer-Verlag 2011

Abstract Toddlers are more prone to develop severe and extrapulmonary tuberculosis (TB) than older children. This is partially explained by differences in the immune response. Early and specific diagnosis is essential to start adequate treatment, especially if the central nervous system (CNS) is involved. The lack of sputum production and inherent dangers or impossibility of sampling CNS lesions may delay diagnosis. In addition, the magnetic resonance imaging (MRI) features of TB abscesses are non-specific and may mimic abscesses of other infectious etiology. ^1H -magnetic resonance spectroscopy (^1H -MRS) may increase specificity of diagnosis by identifying lipids within the lesions that are considered characteristic for TB. Therefore,

we studied four children with presumable CNS-TB with MRI and ^1H -MRS. In vivo and in vitro ^1H -MRS showed elevated lipid peaks within the TB lesions. **Conclusion:** ^1H -MRS allows to non-invasively identifying TB with high specificity and may allow early installment of targeted antimicrobial treatment.

Keywords Cerebral lesions · Diagnosis · Magnetic resonance imaging · ^1H -magnetic resonance spectroscopy · Toddler · Tuberculosis

Introduction

Around one third of the world's population are estimated to be infected with *Mycobacterium tuberculosis* [9], the agent that causes tuberculosis (TB) which is usually transmitted by contaminated air droplets reaching the alveoli [16]. TB disease develops in 10% to 15% of the infected individuals, and the most common type of disease is pulmonary TB [1]. Children younger than 4 years of age and immune-deficient individuals are more prone to most severe forms of TB including extrapulmonary TB (e.g., central nervous system [CNS]) and disseminated TB [14].

Although the number of cases with multi-drug resistant TB is increasing in certain geographic areas [15], it is still largely a curable disease. Anti-tuberculous drug treatment, however, needs to be installed usually for at least 6 months [13]. Thus, a fast and specific diagnosis of TB disease is essential.

Diagnosis of active TB in children, especially in the young ones, is largely hampered by an atypical clinical presentation, young children's incapability to produce sputum, or the difficulty to easily sample the lesions in order to detect and identify *M. tuberculosis* by culture or

K. Santy · P. Nan · Y. Chantana · B. Richner (✉)
Division of Pediatrics, Jayavarman VII Hospital,
Kantha Bopha Children's Hospital,
Siem Reap, Cambodia
beatrichner@online.com.kh

K. Santy
Division of Pediatric Imaging, Jayavarman VII Hospital,
Kantha Bopha Children's Hospital,
Siem Reap, Cambodia

D. Laurent
Division of Pediatric Laboratory Medicine and Microbiology,
Jayavarman VII Hospital, Kantha Bopha Children's Hospital,
Siem Reap, Cambodia

D. Nadal
Division of Infectious Diseases and Hospital Epidemiology,
University Children's Hospital of Zurich,
Steinwiesstrasse 75,
8032 Zurich, Switzerland

D. Nadal
Pediatric Research Center (PRC),
University Children's Hospital of Zurich,
Zurich, Switzerland

molecular methods [19]. Therefore, indirect evidence of *M. tuberculosis* infection including positive results from Mantoux skin testing or interferon γ -release assays is often sought. Nevertheless, the results of these tests rely on the host's immune response to the pathogen and thus may prove inaccurate when the host's immune defense is immature due to young age or impaired, e.g., due to progressed infection with human immunodeficiency virus (HIV) [5]. Thus, novel minimal or non-invasive means to diagnose or confirm TB infection in these individuals are highly desirable.

One of the metabolic hallmarks of *M. tuberculosis* is its production of lipids [6, 16]. These lipids, if in sufficient amounts, can be detected by ^1H -magnetic resonance spectroscopy (^1H -MRS) [4, 12, 17]. Thus, we reasoned that due to its unique capability to detect and characterize lesions in the CNS non-invasively, a combination of magnetic resonance imaging (MRI; anatomical detail) and single voxel ^1H -MRS (biochemical information) of the encountered lesions could provide a valuable means to rapidly establish or confirm the etiologic diagnosis.

We consequently studied four young children with presumable diagnosis of CNS tuberculous infection by MRI and single voxel ^1H -MRS. The hypothesis was tested if lipids are present in TB abscesses. Here, we report that ^1H -MRS enables to clearly discriminate tuberculous from other infectious cerebral abscesses in toddlers. Our findings are of paramount importance to install rapid anti-tuberculous treatment and to monitor its effectiveness.

Patients and methods

Patients The patients reported herein were hospitalized at Jayavarman VII, Siem Reap, one of the five Kantha Bopha Children's Hospitals in Cambodia, in 2009 or 2010 because of severe illness requiring in-patient care. Brain MRI and single voxel ^1H -MRS were done as part of routine diagnostic work-up to investigate the cause for the neurologic deterioration.

Magnetic resonance imaging (MRI) and ^1H -magnetic resonance spectroscopy (^1H -MRS) Imaging was performed on a standard 3 Tesla MR Unit (Philips Achieva 3T, Best, The Netherlands) using the circular polarized multichannel (eight channel) head coil. Conventional imaging included standard, vendor-specific multiplanar T1- and T2-weighted sequences, as well as contrast-enhanced T1-weighted and fluid attenuated inversion recovery (FLAIR) sequences of the brain. The brain was covered from the skull base to the vertex. Single voxel ^1H -MRS (SVS) was performed using a Point Resolved Excitation (PRESS) sequence prior to the contrast-enhanced sequence. The imaging parameters were

TR=2,000 and TE=35 or 144 ms in order to differentiate lipid peaks (0.9–1.3 ppm) from overlapping lactate peaks (1.3 ppm). The number of acquisitions was 128 resulting in an effective ^1H -MRS acquisition time of less than 5 min. The voxel was manually positioned within the encountered focal lesion. Care was given that the voxel did not include adjacent gray or white matter or cerebrospinal fluid (CSF). The voxel size was optimized for the size of the lesion and ranged between 1 and 8 ml; matching and shimming of the sampled volume were performed using the system-specific software. In addition, *in vitro* ^1H -MRS was performed of the aspirated/sampled tissue prior to treatment using the same single voxel PRESS MRS sequence for purpose of comparison. ^1H -MRS was performed within 48 h after sampling. The aspirated material was diluted with 10 ml of saline and contained in a plastic tube. The tube was subsequently positioned in a water container to optimize shimming and matching for data acquisition. The specimen was measured at room temperature. The acquired data were postprocessed after Fourier transformation using the vendor-specific software. The metabolites were calculated as ratios (to creatine); no absolute quantification was performed and displayed along the typical resonance frequency axis.

^1H -MRS was performed in all children with a confirmed TB abscess. In addition, ^1H -MRS was also performed in one child with a confirmed *Streptococcus pneumoniae* brain abscess (reference case).

Laboratory investigations Blood counts, CSF analyses, chemistry, bacterial cultures, and species identification, as well as HIV serology, were done using routine methods. The reference case and all four TB patients were HIV negative. Molecular and culture means to detect mycobacteria were not available.

Clinical assessment The clinical and neurological status was evaluated in all patients prior and after treatment.

Results

Reference case A 7-year-old boy was admitted to the intensive care unit (ICU) because of severe headache and drowsiness. His hematocrit was 34%, total white blood count (WBC) 18.5 G/l, and platelet count 717 G/l. CSF analysis revealed 2 cells/ μl , protein 0.84 g/l (norm<0.5), and glucose 4.4 mmol/l. Brain MRI showed a large brain abscess in the right temporal lobe (Fig. 1a–c). *In vivo* ^1H -MRS of the center of the lesion showed predominant acetate and succinate peaks, no lipids, and only very minimal lactate. These findings are compatible with a

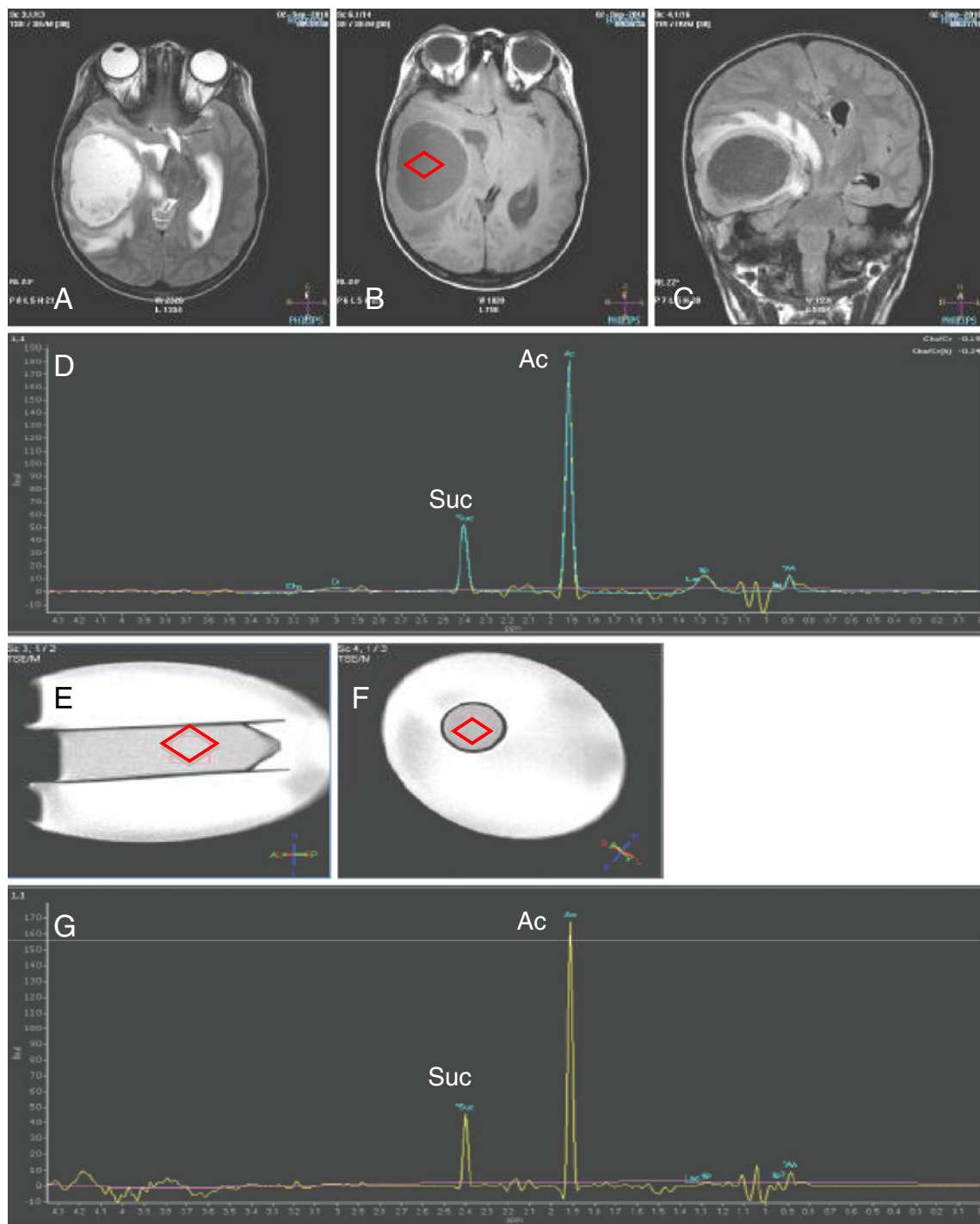


Fig. 1 Brain MRI of a 7-year-old boy (reference case) and ^1H -MRS of pus from cerebral abscess in vivo and in vitro. Axial in T2-weighted (a), T1-weighted (b), and FLAIR (c) MR images reveal a large brain abscess in the right temporal lobe with perifocal edema and mild midline shift. ^1H -MRS of the center of the abscess (d) shows a large acetate (Ac) and smaller succinate (Suc) peak at 1.9 and 2.4 ppm,

respectively, indicating pyogenic abscess. Pus aspirated from the cerebral abscess put in a plastic tube embedded in a water-filled plastic container as depicted by MRI in a lateral view (e) and cross-sectional view (f). In vitro ^1H -MRS of the pus shows the similar resonance peaks (g) as presented in ^1H -MRS in vivo (d). Rhombus symbol indicates where ^1H -MRS was measured

classical non-tuberculous pyogenic abscess (Fig. 1d). In vitro ^1H -MRS of the aspirated pus showed a matching distribution of resonance peaks (^1H -MRS fingerprint; Fig. 1e–g). Bacterial cultures grew *S. pneumoniae*. The child died after 14 days despite treatment with intravenous ceftriaxone. There was no necropsy.

Case 1 A 9-month-old boy was admitted because of generalized muscular hypotonia. Vaccination history for

Bacille Calmette Guerin (BCG) was positive. His hematocrit was 29%, total WBC 26.2 G/l, and platelets 754 G/l. Analysis of CSF revealed 6 cells/ μl , protein 0.3 g/l, and glucose 2.6 mmol/l. Brain MRI showed a large fronto-parietal brain abscess with a small, additional right occipital abscess (Fig. 2a–c). In vivo ^1H -MRS of the center of the lesion showed high lactate and lipid peaks that partially overlapped, along with a small peak of acetate at 1.9 ppm, indicating a bacterial superinfected tuberculous abscess (Fig. 2d). In vitro

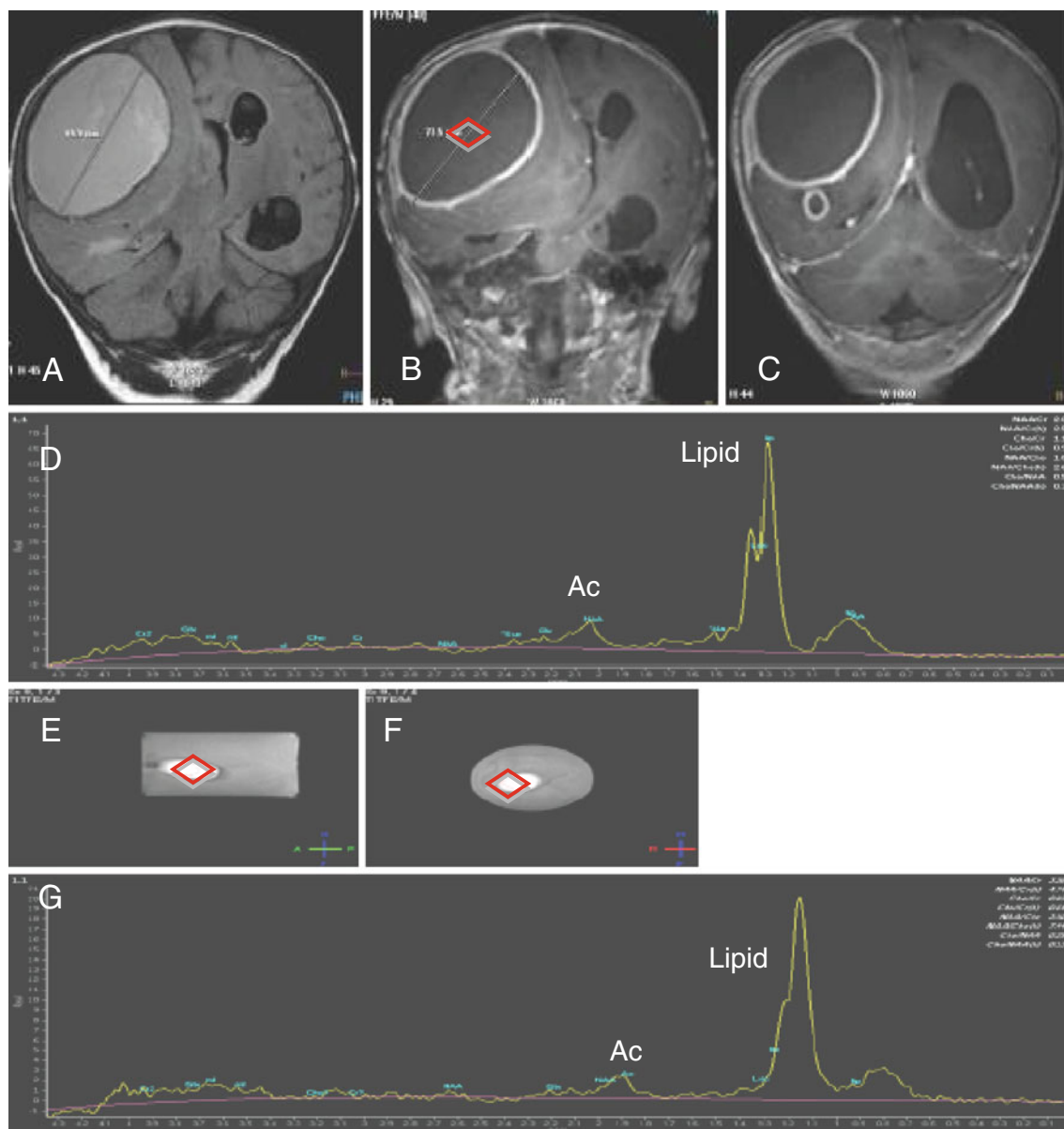


Fig. 2 Brain MRI of a 9-month-old boy (case 1) and in vivo and in vitro ^1H -MRS of the pus from cerebral abscess. Coronal FLAIR (a) and coronal contrast-enhanced T1-weighted (b, c) MR images show a large fronto-parietal brain abscess and a small right parietal abscess. In vivo ^1H -MRS of the abscess center (d) shows a large partially overlapping lactate and lipid peak at 1.3 ppm, along with a small of acetate (Ac) peak at 1.9 ppm. Findings are compatible with a bacterial

superinfected tuberculous abscess. The pus aspirated from the cerebral abscess put in a plastic tube embedded in a water-filled plastic container as depicted by MRI in a lateral view (e) and cross-sectional view (f). In vitro ^1H -MRS of the pus aspirate shows a similar spectrum (spectral fingerprint) (g) as presented in vivo ^1H -MRS (d). Rhombus symbol indicates where ^1H -MRS was measured

^1H -MRS of the aspirated material showed a similar high lactate and lipid peak and a low acetate resonance peak (Fig. 2e–g). Treatment with ceftriaxone, isoniazide, rifampicin, and pyrazinamide plus corticosteroids was started. Bacterial cultures of the aspirated pus remained sterile, but the patient had already received ceftriaxone for 2 days before sampling.

Ceftriaxone was stopped after 15 days. Anti-tuberculous treatment was continued for 12 months, and the patient recovered.

Case 2 A comatose 4-year-old boy who had manifested vomiting and convulsions was admitted to the ICU. Vaccination history for BCG was positive. His hematocrit was 28%, total WBC 12.6 G/l, and platelets 774 G/l. Analysis of CSF revealed 80 cells/ μl , protein 2.4 g/l, and glucose 1.3 mmol/l. Brain MRI showed a left occipital abscess with additional signs of adjacent ependymitis and precipitated material in the left lateral ventricle (Fig. 3a–c). Moderate hydrocephalus with transependymal CSF flow was also noted. The MRI features did not allow differentiating between a bacterial or tuberculous abscess. Subsequent ^1H -MRS of the center of the lesions showed large

partially overlapping lactate and lipid peaks, indicating a tuberculous abscess (Fig. 3d). No additional metabolites were noted. The patient died 14 days later, despite treatment with ceftriaxone, isoniazide, rifampicin, and pyrazinamide plus corticosteroids. There was no necropsy.

Case 3 A comatose 2-year-old boy with convulsions was admitted to our hospital. Vaccination history for BCG was positive. His hematocrit was 34%, total WBC 10.4 G/l, and platelets 473 G/l. Analysis of CSF revealed 46 cells/ μl , protein 5.52 g/l, and glucose 2.0 mmol/l. Brain MRI and ^1H -MRS showed an extensive lepto-meningeal enhancement along the skull base and basal cisterns consistent with a basal meningitis. In addition, multiple solid and cystic lesions were noted within the cerebellum, brainstem, and supratentorial brain (Fig. 4a–c). In vivo ^1H -MRS of the cystic/solid focal lesions showed high lipid peaks compatible with tuberculous lesions (Fig. 4d, e). The solid imposing lesion within the left hippocampus also showed high lipid peaks; however, typical cerebral metabolites like choline, creatine, and *N*-acetylaspartate were also noted. The *N*-acetylaspartate peak was, however, significantly reduced indicating brain injury (Fig. 4f). No in vitro ^1H -MRS was

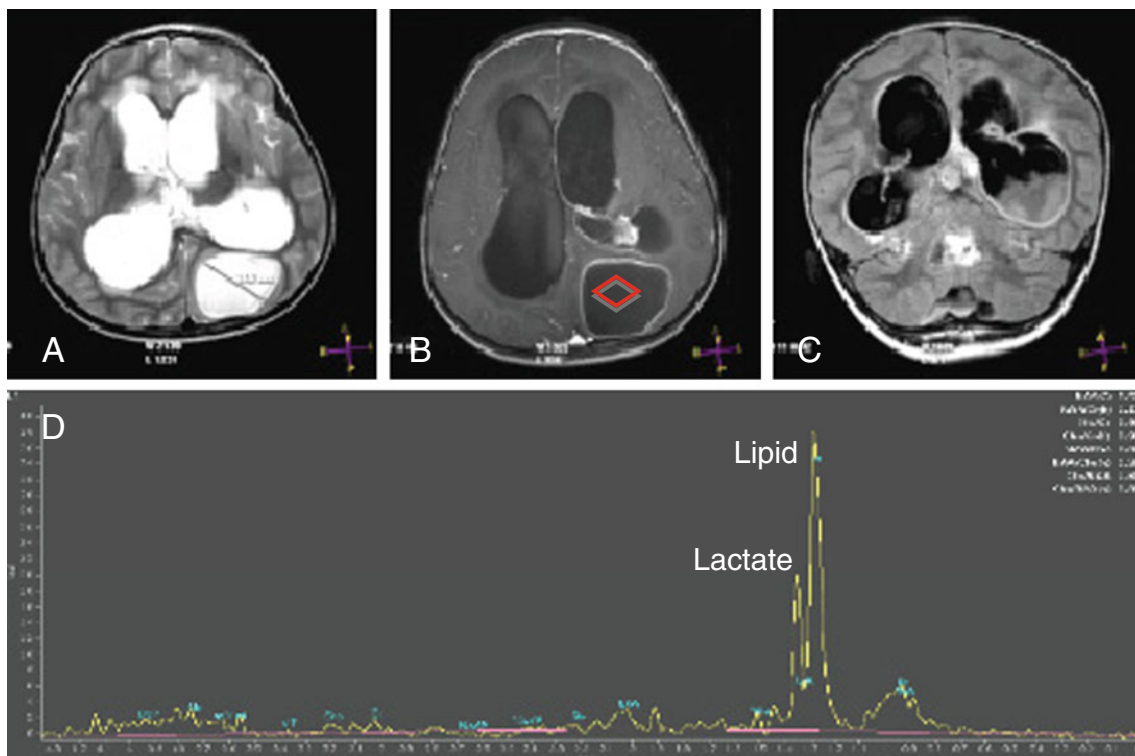


Fig. 3 Brain MRI of a 4-year-old boy (case 2) and in vivo ^1H -MRS of pus from cerebral abscess. Axial T2-weighted (a), contrast-enhanced T1-weighted (b), and coronal FLAIR (c) MR images reveal a large left occipital abscess dorsal to the inflamed lateral ventricle. The ependyma of the ventricle shows a significant contrast enhancement;

in addition, precipitated material is seen in the left lateral ventricle. ^1H -MRS of the center of the pus collection shows a large overlapping lactate and lipid peak (d), indicating likely a tuberculous abscess. *Rhombus symbol* indicates where ^1H -MRS was measured

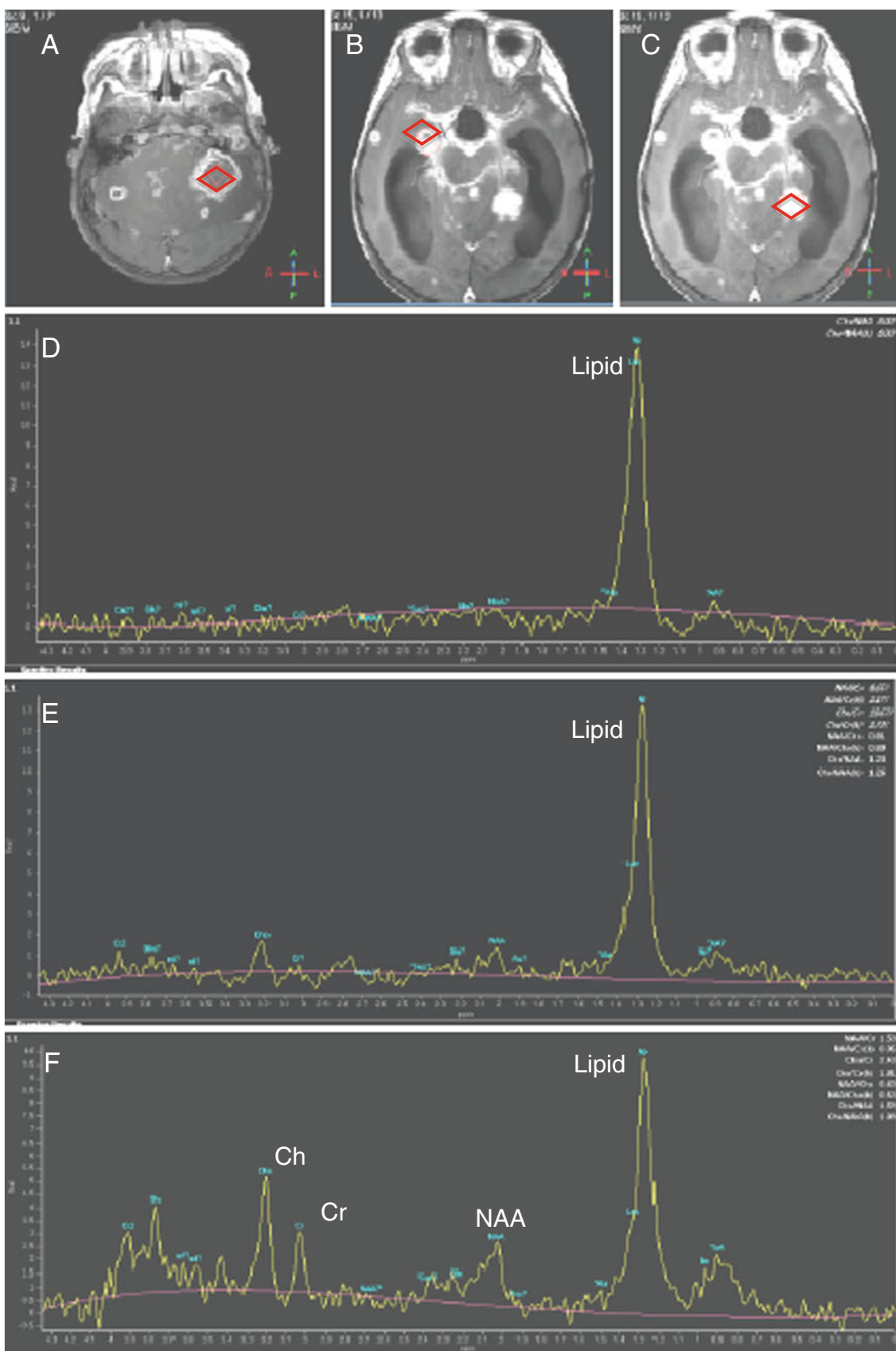


Fig. 4 Brain MRI of a 2-year-old boy (case 3) and in vivo $^1\text{H-MRS}$ of three different intracranial lesions. Axial contrast-enhanced T1-weighted images (a–c [identical to b]) show large left cerebellar hyperintense lesion with ring-like enhancement (a) and a smaller right hippocampal lesion (b, c). In addition, a basal contrast-enhancing meningitis is noted suggestive of tuberculous meningitis. $^1\text{H-MRS}$ show increased lipid peaks in the centrally cystic lesion (d, e). The intraparenchymal, hippocampal lesion shows partially maintained cerebral metabolites (N-acetylaspartate [NAA], Creatine [Cr], and Choline [Ch]) next to a large lipid peak compatible with a tuberculoma. The NAA peak is reduced indicating tissue injury (f). Rhombus symbols indicate where the three $^1\text{H-MRS}$ were measured

available for comparison. The patient died 28 days later, despite treatment with ceftriaxone, isoniazide, rifampicin, and pyrazinamide plus corticosteroids. There was no necropsy.

Case 4 A 3-year-old girl was admitted to our hospital because of severe dyspnea and cervical lymphadenitis. She had no focal neurological symptoms. Her hematocrit was 30%, total WBC 33.5 G/l, and platelets 950 G/l. Analysis of CSF showed 360 cells/ μl , protein 1.23 g/l, and glucose 1.08 mmol/l. Brain MRI showed a T2- and FLAIR hypointense right parieto-occipital periventricular and a midline, vermian lesion with mild perifocal edema (Fig. 5a–c). $^1\text{H-MRS}$ of the focal lesion showed a high lipid peak, without any other metabolites, indicating a tuberculous etiology of the lesions (Fig. 5d). Six months after installment of anti-tuberculous treatment, including isoniazide, rifampin, and pyrazinamide plus corticosteroids, the size of the lesions had decreased by around 50% (Fig. 5e–g). The lipid peak within the lesion persisted, though at a considerably lower level (Fig. 5h). The patient recovered clinically. No in vitro $^1\text{H-MRS}$ was performed.

Discussion

Our data show that lipid peaks are typically seen in tuberculous abscesses, suggesting that $^1\text{H-MRS}$ may help to discriminate between the various infectious etiologies. We show that the $^1\text{H-MRS}$ findings in vivo and in vitro are quite similar in children in whom aspiration of lesion material was feasible. We also show that tuberculous lesions uniformly exhibit elevated lipid peaks by $^1\text{H-MRS}$. Finally, we demonstrate that anti-tuberculous treatment leads to size reduction of cerebral lesions exhibiting lipid peaks. Our findings thus have an important impact on the management of patients with cerebral TB, one of the most severe manifestations of infection with *M. tuberculosis* for which toddlers or immune-deficient patients are at highest risk.

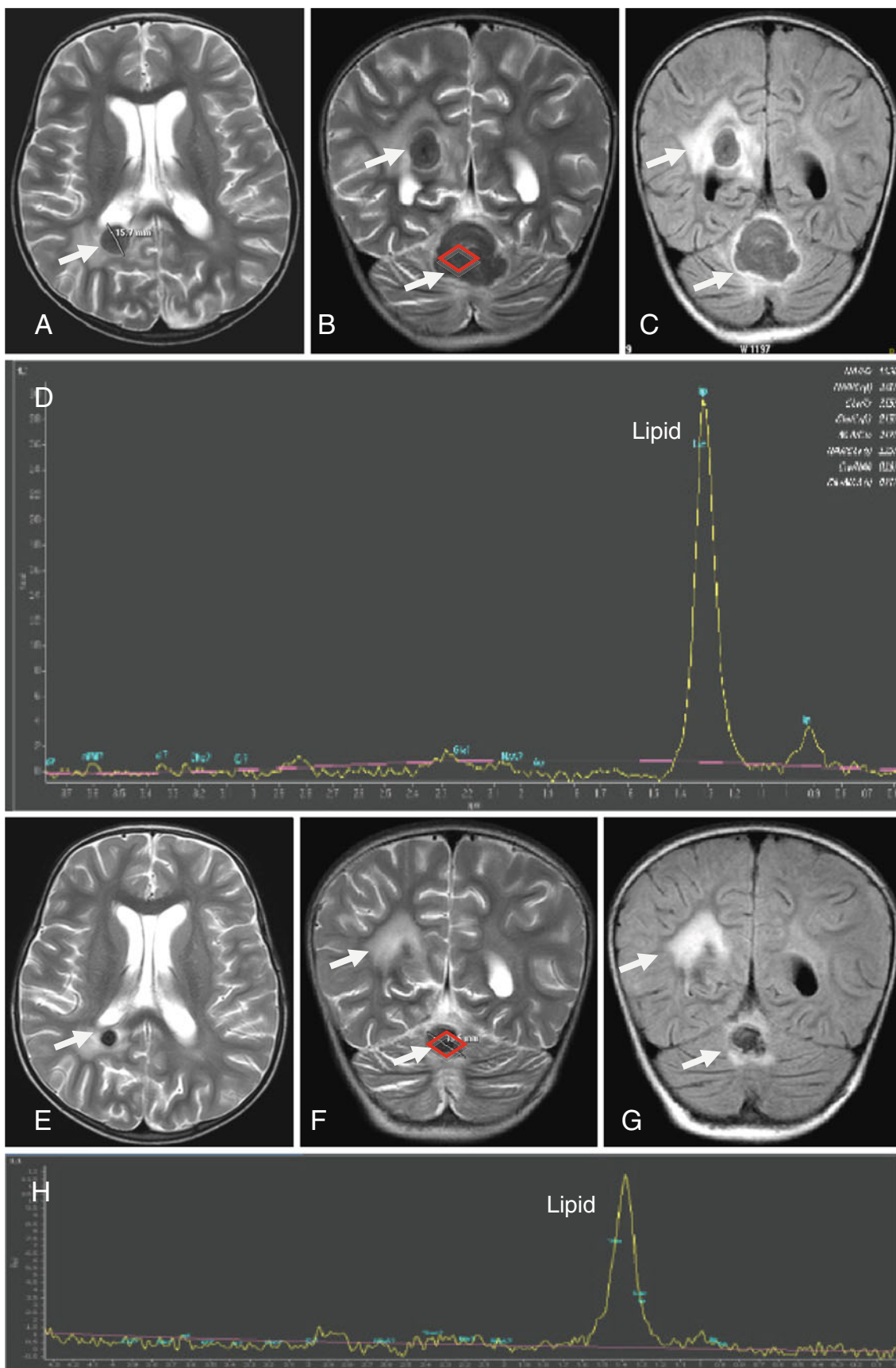
Elevated lipid peaks within the tuberculous lesions as identified by $^1\text{H-MRS}$ permitted to discriminate between tuberculous and non-tuberculous brain lesions. The cell

wall of mycobacteria is predominantly composed of lipids in contrast to that of other bacteria [6, 16]. The lipid resonances at 0.9 and 1.3 ppm are generated by the methylene and terminal methyl groups, respectively, of fatty acids contained in the caseous material [4, 10, 12]. Moreover, there is a relative lack of proteolytic enzymes in the tuberculous inflammatory exudates as compared with pyogenic inflammation [16]. Furthermore, the absence of amino acids at 0.9 ppm in tuberculous abscesses probably is due to the presence of large numbers of tubercle bacilli and the lack of proteolytic enzymes, resulting in poor degradation of proteins into amino acids [16]. On the other hand, acetate and succinate are the end products of fermentation in pyogenic abscesses [4]. Thus, $^1\text{H-MRS}$ exhibiting lipid peaks is highly indicative for tuberculous lesions. As a note of caution, other more rapidly growing bacteria may superinfect tuberculous lesions [18]. This may result in a contamination of the spectrum with appearance of acetate and succinate on $^1\text{H-MRS}$, as shown in case 1 (Fig. 2).

Three of the four children with brain TB underwent BCG vaccination. Of note, vaccination with BCG does not induce so-called sterile immunity and does not reliably prevent pulmonary TB [7]. Though BCG is believed to prevent the most severe forms of childhood TB [7], our observations in this small series and based upon our personal unpublished data of large series of patients infer that this does not hold true. Indeed, the fact that BCG is by far not an ideal vaccine has fueled ongoing efforts towards newer anti-tuberculous vaccines that will hopefully lead to more reliable protection from infection with *M. tuberculosis* [8].

It needs to be stated that our report has the limitation that no attempts were made to detect infection with *M. tuberculosis*, neither directly by culture or molecular methods nor indirectly via immune reactions. Nevertheless, bacterial cultures except for mycobacteria were done from lesion material in the reference case and in case 1, i.e., when material could be collected. In the reference case with absent lipid peak, *S. pneumoniae* grew, whereas there was no bacterial growth in case 1 in whom a lipid peak was present. On the other hand, the considerable regression of lesions exhibiting elevated lipid peaks and reduction of the lipid peak level following treatment with anti-tuberculous drugs for 6 months, as observed in case 4, is compatible with a mycobacterial etiology of the lesions.

Our report on the rapid, specific recognition of tuberculous etiology of focal cerebral lesions in children is unprecedented. The most likely reason for it is the lack of $^1\text{H-MRS}$ in a geographic area highly endemic for TB, although lipid peaks in $^1\text{H-MRS}$ from tuberculous lesions have been known for some time [4, 12]. Areas highly endemic for TB are located virtually in resource-poor



◀ **Fig. 5** Brain MRI of a 3-year-old girl (case 4) and in vivo ^1H -MRS of two brain lesions before and after anti-tuberculous treatment. Axial and coronal T2 and coronal FLAIR MR images prior to treatment show at least two focal, T2-, and FLAIR-hypointense lesions in the left occipital lobe and midline vermis (*arrows*) (**a–c**). In vivo ^1H -MRS prior to treatment show a high lipid peak within the lesion compatible with a tuberculous lesion (**d**). Follow-up axial, coronal T2, and coronal FLAIR MR images after 6 months of anti-tuberculous treatment show a significant reduction in size (>50%) of the tuberculous lesions (**e–g**). The ^1H -MRS again shows a single, high lipid peak within the lesion (**h**). *Rhombus symbol* indicates where ^1H -MRS was measured

countries only [3], where the incidence of TB in toddlers is heavily underestimated [11]. This was well documented by a necropsy study from Africa showing that almost 30% of children younger than 5 years of age who died of acute respiratory disease in fact had undiagnosed TB [2]. Thus, although ^1H -MRS may be regarded as a tool to be reserved for high-technology medical facilities in wealthy countries, our report evidences that it may provide an excellent, non-invasive tool to significantly improve medical care and cure of TB in areas where this is of paramount importance. Our study may indicate that high-technology medical care needs to be brought to resource-poor areas in order to enable coping with human threats such as TB.

Acknowledgments This study was made possible by the Kantha Bopha Foundation that is supported by donations mainly from Swiss people. The authors thank Dr. Ianina Scheer, Prof. Thierry .A. Huisman, and Prof. Beat Steinmann for helpful discussions.

References

- Barry CE 3rd, Boshoff HI, Dartois V, Dick T, Ehrt S, Flynn J, Schnappinger D, Wilkinson RJ, Young D (2009) The spectrum of latent tuberculosis: rethinking the biology and intervention strategies. *Nat Rev Microbiol* 7:845–855
- Chintu C, Mudenda V, Lucas S, Nunn A, Lishimpi K, Maswahu D, Kasolo F, Mwaba P, Bhat G, Terunuma H, Zumla A (2002) Lung diseases at necropsy in African children dying from respiratory illnesses: a descriptive necropsy study. *Lancet* 360:985–990
- Dye C (2006) Global epidemiology of tuberculosis. *Lancet* 367:938–940
- Gupta RK, Vatsal DK, Husain N, Chawla S, Prasad KN, Roy R, Kumar R, Jha D, Husain M (2001) Differentiation of tuberculous from pyogenic brain abscesses with in vivo proton MR spectroscopy and magnetization transfer MR imaging. *AJNR Am J Neuroradiol* 22:1503–1509
- Haustein T, Ridout DA, Hartley JC, Thaker U, Shingadia D, Klein NJ, Novelli V, Dixon GL (2009) The likelihood of an indeterminate test result from a whole-blood interferon-gamma release assay for the diagnosis of *Mycobacterium tuberculosis* infection in children correlates with age and immune status. *Pediatr Infect Dis J* 28:669–673
- Karakousis PC, Bishai WR, Dorman SE (2004) *Mycobacterium tuberculosis* cell envelope lipids and the host immune response. *Cell Microbiol* 6:105–116
- Kaufmann SH (2006) Envisioning future strategies for vaccination against tuberculosis. *Nat Rev Immunol* 6:699–704
- Kaufmann SH (2010) Future vaccination strategies against tuberculosis: thinking outside the box. *Immunity* 33:567–577
- Lonnroth K, Castro KG, Chakaya JM, Chauhan LS, Floyd K, Glaziou P, Raviglione MC (2010) Tuberculosis control and elimination 2010–50: cure, care, and social development. *Lancet* 375:1814–1829
- Luthra G, Parihar A, Nath K, Jaiswal S, Prasad KN, Husain N, Husain M, Singh S, Behari S, Gupta RK (2007) Comparative evaluation of fungal, tubercular, and pyogenic brain abscesses with conventional and diffusion MR imaging and proton MR spectroscopy. *AJNR Am J Neuroradiol* 28:1332–1338
- Marais BJ, Schaaf HS (2010) Childhood tuberculosis: an emerging and previously neglected problem. *Infect Dis Clin North Am* 24:727–749
- Mishra AM, Gupta RK, Jaggi RS, Reddy JS, Jha DK, Husain N, Prasad KN, Behari S, Husain M (2004) Role of diffusion-weighted imaging and in vivo proton magnetic resonance spectroscopy in the differential diagnosis of ring-enhancing intracranial cystic mass lesions. *J Comput Assist Tomogr* 28:540–547
- Mitchison DA, Fourie PB (2010) The near future: improving the activity of rifamycins and pyrazinamide. *Tuberc (Edinb)* 90:177–181
- Newton SM, Brent AJ, Anderson S, Whittaker E, Kampmann B (2008) Paediatric tuberculosis. *Lancet Infect Dis* 8:498–510
- Raviglione MC, Smith IM (2007) XDR tuberculosis—implications for global public health. *N Engl J Med* 356:656–659
- Russell DG (2007) Who puts the tubercle in tuberculosis? *Nat Rev Microbiol* 5:39–47
- Semlali S, El Kharras A, Mahi M, Hsaini Y, Benameur M, Aziz N, Chaouir S, Akjouj S (2008) Imaging features of CNS tuberculosis. *J Radiol* 89:209–220
- Stricker T, Willi UV, Pfyffer GE, Nadal D (1996) A school-girl with constipation. *Lancet* 348:306
- Swaminathan S, Rekha B (2010) Pediatric tuberculosis: global overview and challenges. *Clin Infect Dis* 50(Suppl 3):S184–S194